Cell. Mol. Life Sci. (2010) 67:483–494
DOI 10.1007/s00018-009-0197-x

Cellular and Molecular Life Sciences

RESEARCH ARTICLE

Fusogenic activity of cationic lipids and lipid shape distribution

Caroline Lonez · Marc F. Lensink · Emilie Kleiren · Jean-Marie Vanderwinden · Jean-Marie Ruysschaert · Michel Vandenbranden

Received: 3 September 2009 / Revised: 20 October 2009 / Accepted: 29 October 2009 / Published online: 19 November 2009

Abstract Addition of co-lipids into cationic lipid formulations is considered as promoting cell delivery of DNA by enhancing fusion processes with cell membranes. Here, by combining FRET and confocal microscopy, we demonstrate that some cationic lipids do not require a co-lipid to fuse efficiently with cells. These cationic lipids are able to self-organize into bilayers that are stable enough to form liposomes, while presenting some destabilizing properties reminiscent of the conically shaped fusogenic co-lipid, DOPE. We therefore analyzed the resident lipid structures in cationic bilayers by molecular dynamics simulations, clustering the individual lipid structures into populations of similarly shaped molecules, as opposed to the classical approach of using the static packing parameter to define the lipid shapes. Comparison of fusogenic properties with these lipid populations suggests that the ratio of cylindrical versus conical lipid populations correlates with the ability to fuse with cell membranes.

C. Lonez and M. F. Lensink contributed equally to this work.

C. Lonez (✉) · M. F. Lensink · E. Kleiren · J.-M. Ruysschaert · M. Vandenbranden
Laboratory for Structure and Function of Biological Membranes, Centre for Structural Biology and Bioinformatics, Faculté des Sciences, Université Libre de Bruxelles, CP 206/2, Campus Plaine, Blvd. du Triomphe, 1050 Brussels, Belgium
e-mail: clonez@ulb.ac.be

J.-M. Vanderwinden
Laboratory of Neurophysiology, Faculty of Medicine, Université Libre de Bruxelles, Campus Erasme, CP 601, route de Lennik 808, 1070 Brussels, Belgium

Keywords Fusion · Cationic lipids · Confocal microscopy · Conical shape · Molecular dynamics

Introduction

Cationic lipids are efficient and popular agents to transport efficiently anionic molecules (DNA, RNA, anionic proteins) into cells [1, 2]. Lipoplexes (cationic lipid/DNA complexes) enter into cells mainly via endocytosis [2–4]. Fusion with the plasma membrane is another possible route but has not been directly related to transfection efficiency [2–4]. Addition of some co-lipids, especially the fusogenic phospholipid DOPE, into cationic liposomes improves in vitro delivery of DNA into cells, probably by facilitating fusion events [5, 6]. This hypothesis is mainly based on the fact that the replacement of DOPE by DOPC into cationic liposomes abolishes completely their fusogenic activity with other liposomes or cells, and leads to a decrease of transfection efficiency [5, 7]. Therefore, fusion with the endosomal membrane has, after endocytosis, been suggested as one of the favorite ways to destabilize endosomes, leading to release of lipoplexes into the cytosol [5, 8, 9]. This route avoids degradation of the lipoplexes by lysosomes and might lead to an improvement in the transfection efficiency in vitro [5, 8].

Using a new method combining Förster resonance energy transfer (FRET) and confocal microscopy, we studied fusion of several cationic lipid formulations with macrophage cells by direct visualization. This method allows both localization of lipids into cells and demonstration of lipid mixing with cell membranes by the loss of the FRET signal. Some cationic lipids were shown to fuse very rapidly and efficiently with cells. This fusion was

compared to the one obtained by adding DOPE into a non-fusogenic cationic liposome.

Hypotheses concerning the structures of membrane intermediates involved in the fusion process require lipids exhibiting negative membrane curvature at the junction of the two bilayers [10–12]. Therefore, the fusogenic property of DOPE has been attributed to its conical shape which was evaluated on the basis of its small headgroup size and its ability to adopt an inverted lipid phase above 10°C [6, 13]. The shape of a lipid molecule is classically described by a packing parameter $P = {}^{v}/_{al_c}$ where a, v and l_c are, respectively, the effective head group area, the hydrocarbon volume and the critical length of the lipid tail [14, 15]; deviation of P from unity has been considered as a way to decide whether non-lamellar aggregates can be expected. This static and geometrical description did not consider the dynamical behavior of lipids: in a lipid aggregate one lipid does not adopt a well-defined and unique structure and the effective shape is a result of the distribution of lipid populations, which is influenced by the constraints imposed by the surroundings. Furthermore, this method considered that cone-shaped lipids (fusogenic) could only form an inverted-micellar structure and suggested that bilayer formulations are not favorable for fusion. Here, we characterize with molecular dynamics simulations the lipid populations of several cationic bilayers by accumulating individual and uncorrelated lipid structures over the course of the simulations. Interestingly, this method demonstrates that cylindrically and conically shaped cationic lipids can co-exist in the same bilayer. By comparing fusogenic behavior with lipid populations, we demonstrate that a shift in populations from cylindrically to conically shaped lipids in lipid bilayers correlates with a strong tendency to fuse with cell membranes.

Materials and methods

Reagents

Texas Red® 1,2-dihexadecanoyl-sn-glycero-3-phosphoethanolamine, triethylammonium salt (Texas Red-DHPE), *N*-(7-nitrobenz-2-oxa-1,3-diazol-4-yl)-1,2-dihexadecanoyl-sn-glycero-3-phosphoethanolamine, triethylammonium salt (NBD-PE) and TOTO®-3 iodide are Invitrogen (Molecular Probes) products. 1, 2-Dioleoyl-3-trimethylammonium-propane chloride salt (DOTAP) and 1,2-dioleoyl-sn-glycero-3-ethylphosphocholine (chloride salt) (EDOPC) were purchased from Avanti Polar Lipids. 1,2-Ditetradecanoyl-rac-glycerol-3-phosphocholine (DMPC) was purchased from Sigma-Aldrich.

DiC_{14}-amidine (3-tetradecylamino-*N*-*tert*-butyl-*N*′-tetradecyl-propionamidine) was synthesized as described [16] and DiC_{16}-amidine (3-tetradecylamino-*N*-*tert*-butyl-*N*'-hexadecyl-propionamidine) was synthesized following the same protocol.

Liposome preparation

Lipids were dissolved in chloroform with 0.8 mol% of each fluorescent probes (Texas Red-PE and NBD-PE). After lipid film formation (by solvent evaporation under nitrogen stream), lipids were resuspended in filtered Hepes 10 mM at 55°C. Liposomes were then stored at 4°C and heated at 55°C for 10 min just before the experiment.

Cell handling

RAW 264.7 macrophage cell line was cultured in DMEM (Invitrogen) supplemented with 10% FBS (Biowhittaker), 1 mM sodium pyruvate, 1 mM glutamine and antibiotics (Invitrogen) (Complete Medium). P388D1 macrophage-like cell line was cultured in RPMI (Invitrogen) supplemented with 10% FBS (Biowhittaker), 1 mM sodium pyruvate, 1 mM glutamine and antibiotics (Invitrogen) (Complete Medium).

Lipid mixing assay

Fusion between cationic liposomes and P388D1 cells was monitored using fluorescence resonance energy transfer assay (FRET) as described [17, 18]. A cell suspension was prepared after washing 2 times with PBS-D, and diluted to 10^6 cells/ml in PBS-glucose (PBS-D from Invitrogen + 1 mg/ml glucose). Cells were kept on ice until use and equilibrated at 37°C in the fluorimeter cuvette before measurement. Cationic liposomes containing NBD-PE and Texas Red-PE at 0.8% each (molar ratio) were used to prepare liposomes as described above. Then, 18.5 nmol of cationic liposomes or neutral liposomes were added to 1 ml of cells. The samples were gently stirred throughout the experiment. The fluorescence was monitored using an SLM-8000 spectrofluometer with excitation and emission slits of 4 nm. Generally, samples were excited at 470 nm and emission spectra were recorded between 500 and 625 nm. Control emission spectra were performed in parallel before and after fusion. The initial fluorescence of the labeled liposome suspension was recorded as 0% fluorescence (F_0) and the 100% fluorescence was determined after adding Triton X-100 at 0.1% (v/v) final concentration (F_{100}). Percentage of fusion was estimated from the fluorescence of NBD at 535 nm (F_{NBD}): $\%F = \frac{(F_{NBD}-F_0)}{(F_{100}-F_0)}$.

Confocal microscopy

After three rinses in PBS buffer and fixation of cells with 4% paraformaldehyde (PAF) in PBS, coverslips were

mounted with FluorSave™ (Calbiochem) before viewing under a LSM510 NLO META confocal microscope fitted on an Axiovert M200 inverted microscope equipped with a C-Apochromat 40×/1.2 N.A. water immersion objective (Zeiss, Jena, Germany).

For detection of the fluorescence resonance energy transfer (FRET), single optical sections, 2 μm thick, were collected and analyzed with the META™ spectral analyzer (width 490–693 nm, by 10-nm steps) under constant hardware settings.

Emission maxima at 530 and 605 nm, respectively, were in agreement with the literature [19, 20]. The 458-nm excitation wavelength of the Argon/2 laser was used to excite the donor fluorochrome (NBD). Laser power and PMT gain were set to generate a robust signal of the donor alone. Under such settings, autofluorescence of the cells (i.e., in absence of any fluorochrome) and direct excitation of the acceptor were minimal. Presence of the acceptor (Texas Red) was confirmed using the 543-nm excitation wavelength of the HeNe1 laser, a main dichroic HFT 488/543/633 and a long-pass emission filter (LP560 nm). The appearance of an emission maximum peak at 605 nm (Texas Red), associated with a small peak at 530 nm (NBD), is the spectral signature of FRET occurrence within the donor/acceptor pair. Images (2,048 × 2,048 pixels, pixel size: 0.1125 μm) were displayed and emission spectra for regions of interest (5 pixels spots) were analyzed with the Zeiss LSM510 software (version 3.2SP2). Figures were generated using ImageJ software.

Modeling setup and equilibration

Molecular dynamics simulations were performed with the Gromacs 3.3 package [21], using the OPLS/aa force field [22], with Berger parameters for the lipid tails [23]. The simulation boxes for DMPC and diC_{14}-amidine were obtained from the final frames of our previously published diC_{14}-amidine:DMPC mixed simulation studies [24]. All simulation parameters, including amidine head group charges, were taken as before [24], unless mentioned otherwise. Simulations were run at a temperature of $T = 310$ K and for a period of 40 ns. Virtual interaction sites were used to remove angular vibrations involving hydrogens, allowing for a time step of 4 fs [25]. Head group charges of the other lipids in the study (PC and TAP) were derived similarly as before [24], by fitting atomic point charges to reproduce the electrostatic potential obtained from ab initio HF/6-31G* calculations [26], keeping symmetry considerations [27, 28]. The DOTAP simulation box was obtained from an initial box of 128 POPC lipids (downloadable from http://moose.bio.ucalgary.ca/files/popc128a.pdb), of which the palmitoyl chain was extended by two carbons to obtain the required oleoyl length. The space for the extra carbons was obtained by shifting each bilayer leaflet by 1 Å outwards. The PC head group was mutated into TAP by first removing the head group, and then building TAP such that the $N(CH_3)_3$ group was always directed away from the bilayer center. The original water molecules were taken to solvate the box, augmented by additional water molecules to fill the vacuum that is formed after the effective removal of the phosphate group, avoiding placement in between the two innermost water molecules from the original set. Of the newly added water molecules, 128 were randomly replaced by Cl^- counterions [29] to obtain electrostatic neutrality. The system was equilibrated with 1,000 steps steepest descent energy minimization and 10 ps free MD. The diC_{16}-amidine simulation box was obtained using the following protocol: a single lipid was built with extended chains, and then multiplied and mirrored in the x and y, and z direction, respectively, to obtain a final system size of 8 × 8 × 2 lipids. This system was protonated and energy minimized in vacuo, and subsequently solvated with 6,340 TIP4P [30] water molecules of which 128 were randomly replaced by Cl^-. The solvated system was minimized by running 1 ns free MD.

Binding times of monovalent cations like Na^+ to lipids are in the order of 25 ns, with the slowest step the diffusive process through the generally positively charged headgroup region to bind the carbonyl and phosphate groups [31–33]. Binding of chloride ions to phospholipid bilayers is significantly faster because they are found to bind the solvent-accessible choline groups in the case of DMPC [24, 33, 34], and to partly remain in the solvent phase in the case of diC_{14}-amidine [24]. Analogous to PC lipids, counterions in a DOTAP bilayer are expected to ultimately bind the choline groups, and they were therefore already placed in the vicinity. In the case of the newly created diC_{16}-amidine bilayer, Cl^- counterions are expected to partly remain in the solvent phase. In conclusion, in both cases (DOTAP and diC_{16}-amidine), equilibration should occur relatively quickly. The area per lipid was used as a qualification of the equilibration of the system and was found to fluctuate around its final equilibrium value within the first 10 ns of the simulation. This fact is confirmed by an investigation of the counterion density along the bilayer normal and over various time ranges during the simulations (data not shown). We therefore used the final 30 ns of the simulations for analysis in all cases.

Clustering

Individual time frames and lipid structures of the simulation were concatenated into an extended lipid "trajectory" ($\Delta t = 100$ ps), that was pruned by keeping only every 9th lipid, resulting in a lipid "trajectory" of 4,435 lipids. This

procedure includes all individual lipid molecules, but also avoids correlation between the same lipid molecules in neighboring time frames (with 64 lipids in each monolayer, a lipid molecule originating from time frame t is not included again until time frame $t + 900$ ps). The root mean square deviation (RMSD) of every lipid structure pair was calculated, using only the acyl chain carbon atoms. Clustering was performed on the basis of this RMSD matrix [35], increasing the RMSD cut-off in steps of 0.01 nm until the two largest clusters together contained 80% of all lipid structures. Distribution-free energies of the clusters were calculated from the relative size of each cluster, assuming a Boltzmann distribution of lipid structures. Lipid structures deviating more than half the RMSD cut-off with the rest of the cluster were saved and are depicted in Fig. 8 (see below). We define the ratio of cylindrically (C) versus conically (V) shaped lipid cluster populations as $R_{C/V} = N_C/N_V$, where N is the number of lipid structures in the respective cluster.

Results

DiC_{14}/diC_{16}-amidine liposomes fuse with macrophages cell line P338D1

DiC_{14}-amidine liposomes fuses with lipoproteins [36], and phospholipid liposomes [24, 37], but fusion with a cellular system has not been demonstrated so far, even if transfection experiments and endosome disruption suggested this activity [38]. We therefore examined fusion of cationic liposomes with P388D1 cells at 37°C by monitoring the transfer of fluorescence energy (FRET) between two probes inserted into the liposomes. DiC_{16}-amidine and diC_{14}-amidine liposomes fuse very rapidly with cells (Fig. 1) whereas DOTAP, EDOPC as well as phospholipid liposomes (DMPC) do not show any fusogenic activity (Fig. 1). Neither the length of the hydrocarbon chains, nor the transition temperature (respectively 23 and 37°C for diC_{14} and diC_{16}-amidine) seems to be a determining factor in the capacity of the liposomes to fuse. A predominant role in the fusion mechanism may therefore lie in the amidine head group or in the lipid shape as was previously suggested [6].

Localization of lipids into cells by confocal microscopy

To localize cationic lipids into cells after fusion and to visualize fusion with cell membranes, we combined FRET and confocal microscopy (Fig. 2). P388D1 incubated 30 min with labeled diC_{14}-amidine liposomes were analyzed using the laser excitation at 458 nm (in the excitation spectra of NBD). DiC_{14}-amidine liposomes fused with cell membranes after 30 min incubation, as demonstrated by the disappearance of FRET [absence of Texas Red emission, in red, emission of green fluorescence characteristic of the donor (NBD)] (Fig. 2). Furthermore, the fluorescence diffused massively inside cells (with an exception for the nucleus), suggesting that diC_{14}-amidine liposomes fused with the intracellular membranes network.

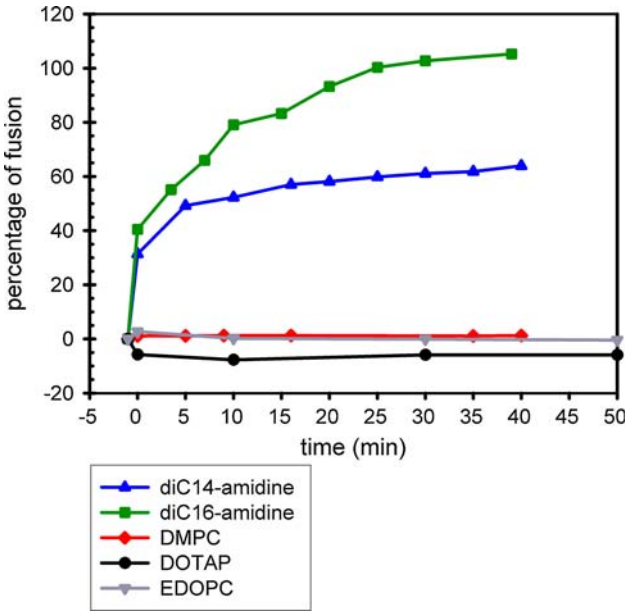

Fig. 1 Fusion between cationic liposomes and cells in suspension (P388D1 cells) in a quartz cuvette thermostatized at 37°C in PBS buffer. Cationic liposomes are labeled with two fluorescent probes, NBD-PE (donor) and Rh-PE (acceptor) in such a concentration that the fluorescence of the donor is transferred to the acceptor. P388D1 cells were then incubated with these liposomes and emission spectra were monitored for 40 min using a spectrofluorimeter as described under "Materials and methods". Percentage of fusion was then calculated using the increase of the fluorescence of the donor (NBD, at 530 nm) as the signature of a lipid mixing. The data are representative of at least four separate experiments

To ensure that the green fluorescence is due to lipid mixing and that autofluorescence of cells cannot be mistaken for NBD fluorescence (same spectral region), we performed a control experiment (Fig. 3) where all the observations were made simultaneously on the same microscope field in order to exclude possible differences in light absorption efficiency between different fields. Furthermore, the confocal microscope was equipped with META^{TM} spectral analyzer (Zeiss) which records the emission spectrum for each pixel, allowing the analysis of the emission spectra at specific spots in cells and the quantitative assessment of FRET efficiency (Fig. 3, bottom left).

Cells were divided in four groups. The first group (autofluorescence control: group 1) was treated with the nucleus stain TOTO-3 only. The second and the third groups of cells were treated 30 min with diC_{14}-amidine liposomes labeled

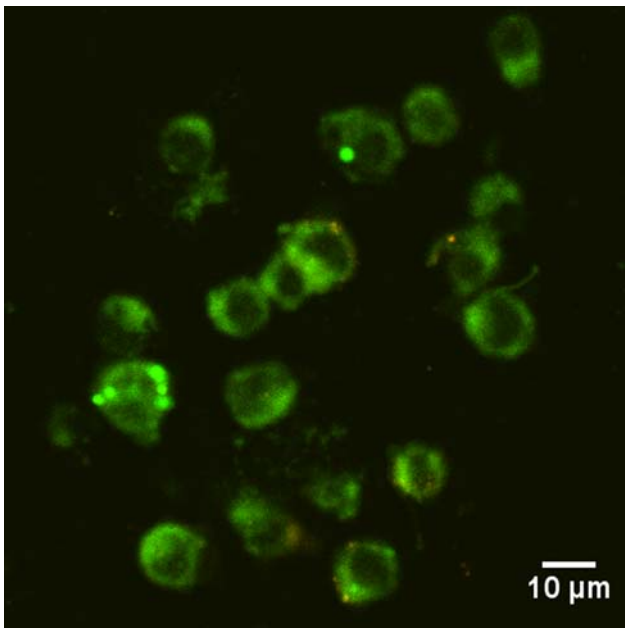

Fig. 2 Fusion between diC_{14}-amidine liposomes and P388D1 cells. P388D1 were incubated 30 min with diC_{14}-amidine liposomes labeled with Texas Red-PE and NBD-PE. After fixation, cells were analyzed with a LSM510 NLO META confocal microscope using the 458 nm excitation wavelength to excite the donor fluorophore. The data are representative of two separate experiments

with either NBD-PE (group 2) or Texas Red-PE (group 3). The last group was treated with double-labeled (Texas Red-PE and NBD-PE) diC_{14}-amidine liposomes for 30 min (group 4). After fixation, cells were mixed and analyzed with the confocal microscope using the 458 nm excitation wavelength (left) or different wavelengths together (458, 543, 633) to excite the different probes (right). By exciting the three probes separately, we were able to identify the different groups of cells into the mix. Using the 458-nm excitation laser on the first group (1+2+3+4), we could only detect green fluorescence in cells (Fig. 3, left). The settings were adjusted to minimize the green autofluorescence in group 1 (control) cells which was significantly weaker than the NBD green fluorescence. When excited at 458 nm, control cells (1) and Texas Red-labeled (3) were not visible while NBD-labeled cells (2) and NBD/Texas Red-labeled cells (4) were both detected through their green fluorescence (Fig. 3, left). The absence of energy transfer to the Texas Red probe is not due to degradation/loss of this marker after liposome uptake by cells since it is still visible when excited in its absorption band with the 543 nm laser (Fig. 3, right). Together with the spectral analysis of different cells (bottom left), showing the decrease of the Texas Red peak (around 605 nm) and the increase of the NBD peak (around 530 nm), as compared to non-fused liposomes, it demonstrated clearly that double-labeled diC_{14}-amidine liposomes (4) have fused with most of cell membranes.

Study of the spontaneous fusion of liposomes with cells was also studied by confocal FRET microscopy on RAW 264.7 cells. The larger size of these cells and their adherent properties facilitate the comparison between different lipid formulations.

RAW 264.7 cells were treated for 30 min with different lipid formulations (cationic or neutral), labeled with both NBD and Texas Red-PE, and analyzed on the confocal microscope (Fig. 4) and spectral analyzer using the 458 nm laser (Fig. 5). As with P388D1 cells, diC_{14}-amidine liposomes efficiently fuse with cell membranes, as suggested by the green fluorescence inside cells (Fig. 4a, b).

The spectral analysis (Fig. 5a, b) also confirmed that, inside cells, diC_{14}-amidine liposomes have fused with cell membranes, while, at the periphery or outside cells (red spots outside cells), liposomes of diC_{14}-amidine still present resonance energy transfer between fluorescent probes. The same conclusions can be made for diC_{16}-amidine liposomes, which, like diC_{14}-amidine, fuse efficiently with cells (Figs. 4 and 5e). In contrast, the rare red spots, not localized into cells, in the case of DMPC liposomes illustrate the poor uptake of these neutral liposomes by cells (Figs. 4 and 5f). The distribution pattern and the spectral characteristics of non-fusogenic cationic lipids (DOTAP and EDOPC) are also clearly different (Figs. 4 and 5c, and 4 and 5d). Fusion is largely marginal, as illustrated by the red/yellow spots localized all around the cells (Fig. 4c, d) and suggesting that, in contrast to diC14-amidine, DOTAP or EDOPC liposomes are probably mainly taken up by endocytosis.

We performed the same experiment but using liposomes of DOTAP containing 20% (molar ratio) of a frequently used co-lipid, DOPE. Obviously, addition of DOPE into DOTAP liposomes leads to an efficient fusion with cell membranes (Fig. 6). This latter result confirms (1) the role of DOPE in cationic liposomes fusion, (2) the fact that some cationic lipids do not require the addition of a co-lipid to fuse efficiently, and (3) validates our technique to detect membrane fusion between cationic liposomes and cells.

Does the distribution of lipid shapes into cationic lipid bilayers correlate with their fusogenic properties?

It is generally stated that fusion between lipid membranes is induced by conically shaped lipids (see "Introduction"). We therefore performed molecular dynamics simulations to identify lipid shape distribution present in cationic lipid bilayers and to find a possible correlation with the fusogenic properties observed in the fluorescence experiments. Figure 7 shows the area per lipid, calculated during the course of the simulation. After an initial equilibration period (10 ns), fluctuations of the area per lipid lie within 5 Å and are well within acceptable bounds. Both the

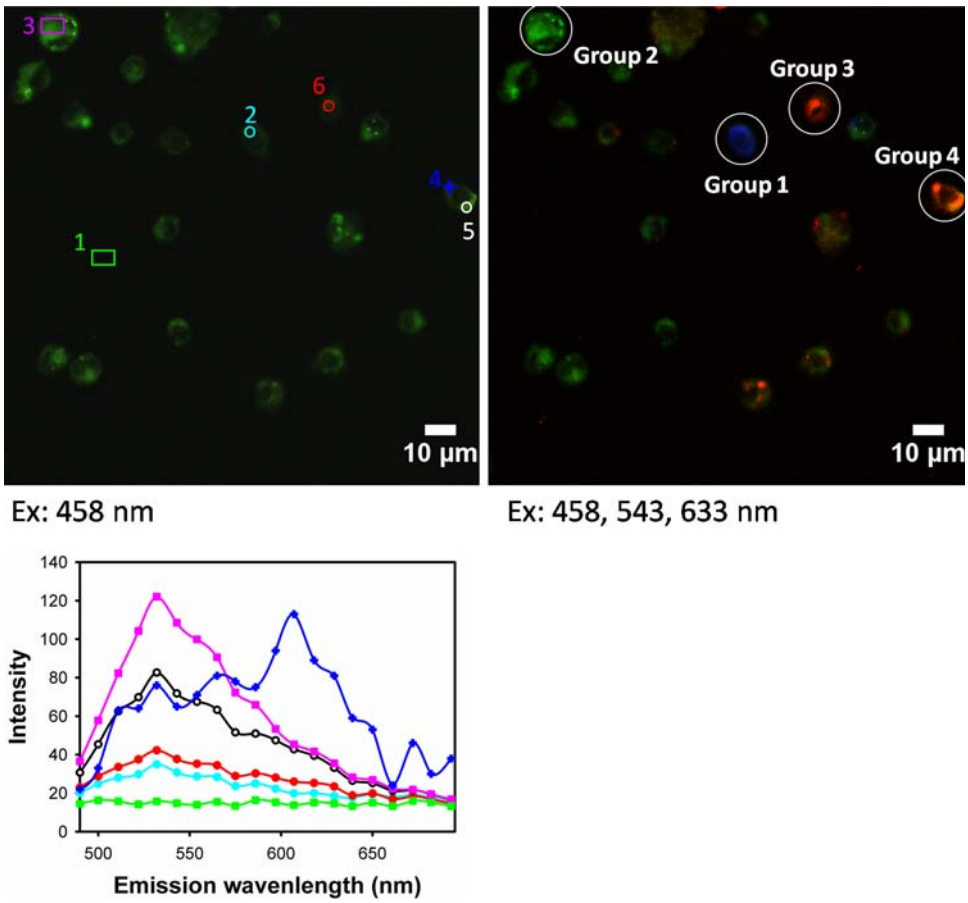

Fig. 3 Comparison of the fusogenic properties of diC_{14}-amidine liposomes with P388D1 cells. P388D1 were incubated 30 min with different conditions. *1* Control cells stained with TOTO-3, *2* cells incubated with diC_{14}-amidine/NBD-PE, *3* incubated with diC_{14}-amidine/Texas Red-PE liposomes, *4* cells incubated with diC_{14}-amidine/NBD-PE/Texas Red-PE. After fixation by 4% PAF, the different groups were mixed (groups 1+2+3+4) and analyzed with a LSM510 NLO META confocal microscope and spectral analyzer using the 458-nm excitation wavelength to excite the donor fluorophore (and detect energy transfer) or using the 458, 543, and 633 nm lasers together to excite the different probes directly. Regions of interest for emission spectra analysis inside cells are indicated by *crosses* or *boxes*. The data are representative of two separate experiments

diC_{14}-amidine and DMPC simulations show average values that are consistent with previous simulations [24] and experimental values [39], respectively. No reference values exist for diC_{16}-amidine or DOTAP, but the figure shows no trend deviating from the calculated average, and the parameter calculation is consistent over the four simulations. In addition, previous molecular dynamics simulations of DMTAP cationic bilayers have found an increased area per lipid with respect to non-cationic bilayers, that lies in the range of 0.7 nm^2 [40]. We therefore conclude that our simulations are sufficiently equilibrated and perform the clustering of the individual lipid structures into populations of similarly shaped molecules over the trajectory range 10–40 ns.

The main clusters of every bilayer simulation are depicted in Fig. 8. In all instances, the main cluster correspond to straight-tailed lipids (cylinder), the second cluster to a V-shaped population (cone), and the third cluster represents twisted-tail lipids (twist). Together, the three clusters represent close to 90% of all lipid structures in the bilayer. Interestingly, this method demonstrates that cylindrically and conically shaped cationic lipids can co-exist in the same bilayer. Overall, the populations are not too different between lipid species, which correlates with the fact that the main lipid populations depict similarly shaped lipids and that, in all cases, a bilayer system is simulated. However, upon closer investigation, a shift in population between cylindrically (C) and conically (V) shaped, i.e., the first and second most frequent lipid populations, can be observed: for diC_{14}- and diC_{16}-amidine lipids (both fusogenic), the population of C lipids has decreased by 5%, compared to DMPC and DOTAP (both non-fusogenic), largely in favor of the V-shaped lipid population. A 3–5% shift of lipids from cylindrical to conical is a non-negligible percentage; it should be kept in mind that the lipid clusters are calculated from a population analysis in a bilayer structure and therefore do not represent an intermediate structure of a fusogenic process, since, per se, membrane fusion implies (at least) a local loss of the bilayer structure. What we therefore observe is rather a tendency of lipids to form specific structures that are commonly accepted to help the membrane to curve at the fusion contact point. This value could be constrained within a very narrow zone with on one side a fusogenically inert bilayer (as pure DOTAP and DMPC) and on the other a too unstable bilayer to form viable liposomes (as pure DOPE).

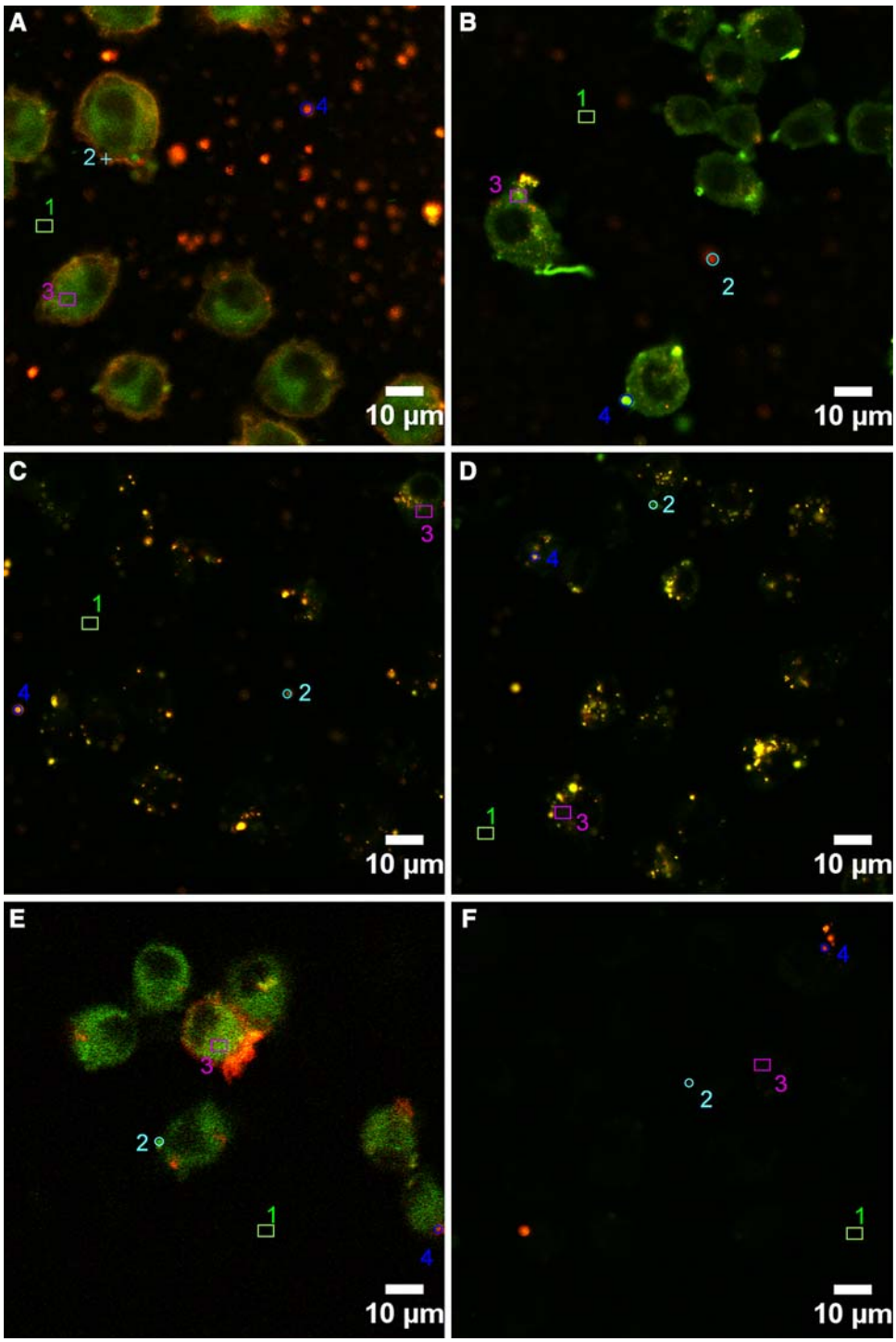

Fig. 4 Fusogenic property of different liposomal formulations with adherent macrophages: confocal images. RAW 264.7 cells were incubated for 30 min (**b**–**f**) or 5 min (**a**) with diC_{14}-amidine (**a** and **b**), DOTAP (**c**), EDOPC (**d**) diC_{16}-amidine (**e**) or DMPC (**f**) liposomes labeled with 0.8 mol% of NBD-PE (donor) and Texas Red-PE (acceptor). Regions of interest for emission spectra analysis inside cells (indicated by *circles*, *crosses* or *boxes*) were analyzed using a LSM510 NLO META confocal microscope and spectra analyzer. Respective data were plotted in Fig. 5. The data are representative of at least three separate experiments

The ratio of cylindrical versus conical lipids, quantified in $R_{C/V}$, may be a determining parameter for fusogenic behavior. Its value lies above four for the non-fusogenic lipids DMPC and DOTAP, while it is well below four for the fusogenic amidine lipids. Therefore, it is possible that a threshold value exists for $R_{C/V,}$ below which the tendency to form V-shaped lipid structures shifts the liposomes into fusogenic behavior. The addition of DOPE to DOTAP may have decreased the $R_{C/V}$ value below this threshold, by shifting the lipid populations in the DOTAP/DOPE liposome towards a fusion-favorable equilibrium (Fig. 6).

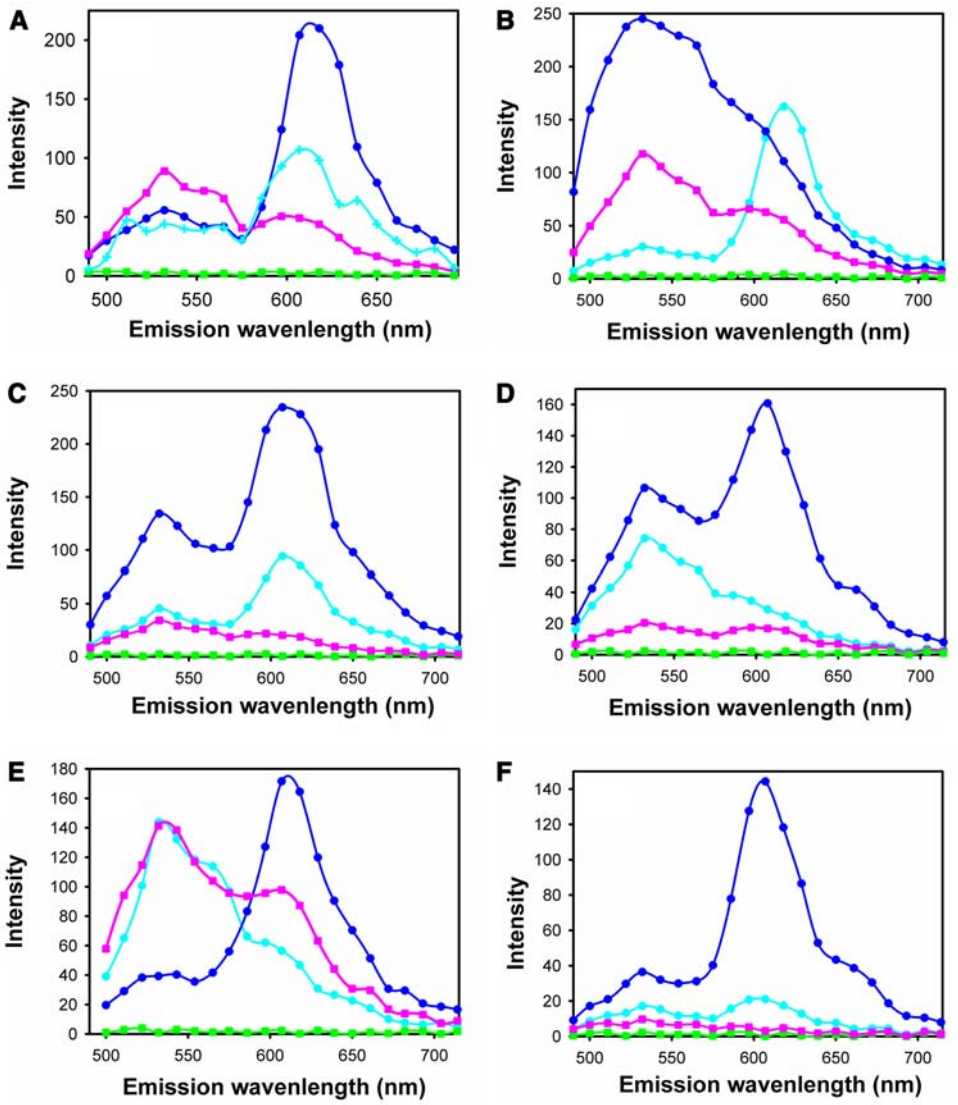

Fig. 5 Fusogenic property of different liposomal formulations with adherent macrophages: emission spectra analysis. RAW 264.7 cells were incubated for 30 min (**b**–**f**) or 5 min (**a**) with diC_{14}-amidine (**a** and **b**), DOTAP (**c**), EDOPC (**d**) diC_{16}-amidine (**e**) or DMPC (**f**) liposomes labeled with 0.8 mol% of NBD-PE (donor) and Texas Red-PE (acceptor). Regions of interest for emission spectra analysis inside cells (indicated by *circles*, *crosses* or *boxes* in Fig. 4) were analyzed using a LSM510 NLO META confocal microscope and spectra analyzer. The data are representative of at least three separate experiments

Discussion

We have demonstrated here that diC_{14}-amidine and diC_{16}-amidine cationic lipids fuse very efficiently and rapidly with cells (Fig. 1). A method, based on an extension of the classical FRET monitoring of liposome fusion to the observation of individual cells by confocal microscopy, was used to show qualitative and quantitative differences in behavior between liposomal preparations that could not be seen otherwise (Figs. 2, 3, 4 and 5). This method allows the localization of cationic lipids into cells and demonstrates that any observed insertion of cationic lipids into cell membranes is the result of lipid mixing between cell lipids and liposomes.

It is generally accepted that fusogenicity, as well as membrane instability, may be promoted by the so-called inverted conical shape of selected lipids [6]. Some of these lipids, like the unsaturated phosphatidylethanolamine, with a small hydrophilic headgroup and a large two-tailed hydrophobic part, impose a negative curvature on the bilayer and favor a transition to non-bilayer phases such as hexagonal, inverted micellar or rhombohedral phases [6, 41]. As such, they are incompatible with liposome formation in many circumstances and should therefore be mixed with a bilayer-forming lipid.

Using the FRET/confocal microscopy technique, we tested the effect of DOPE insertion into non-fusogenic DOTAP liposomes. Addition of DOPE to DOTAP liposomes led to a fusion as efficient (Fig. 6) as the one observed with diC_{14} and diC_{16}-amidine alone (Fig. 4). We therefore provide experimental evidence that fusogenicity of cationic lipids does not necessarily require the addition of a fusion-enhancing co-lipid. One possible explanation is that diC_{14} and diC_{16}-amidine possess an intrinsic propensity to

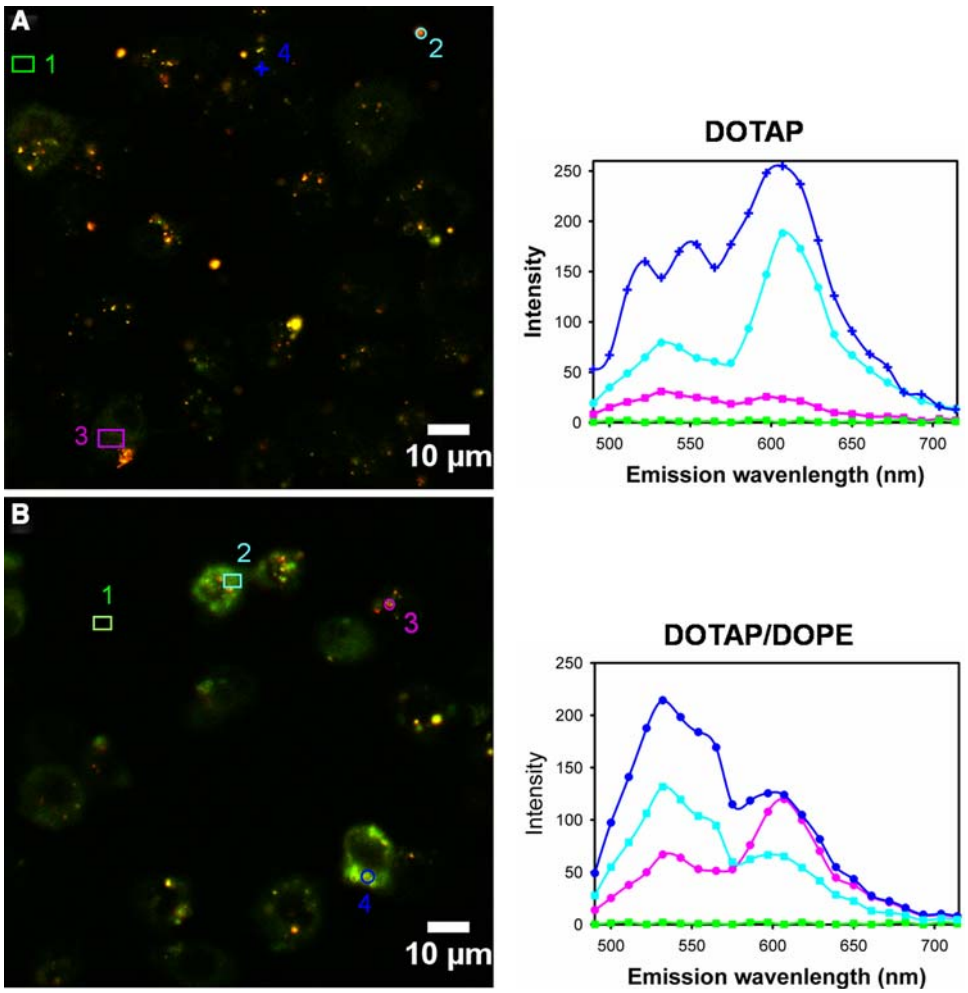

Fig. 6 Addition of DOPE to DOTAP liposomes improves fusion with RAW 264.7 cells. RAW 264.7 cells were incubated for 30 min with labeled (0.8 mol% of NBD-PE and Texas Red-PE) DOTAP liposomes containing or not 20% (molar ratio) of DOPE. Region of interest for emission spectra analysis inside cells (indicated by *circles*, *crosses* or *boxes*) were analyzed using a LSM510 NLO META confocal microscope and spectra analyzer. Respective data were plotted to the right of the respective confocal image. The data are representative of three separate experiments

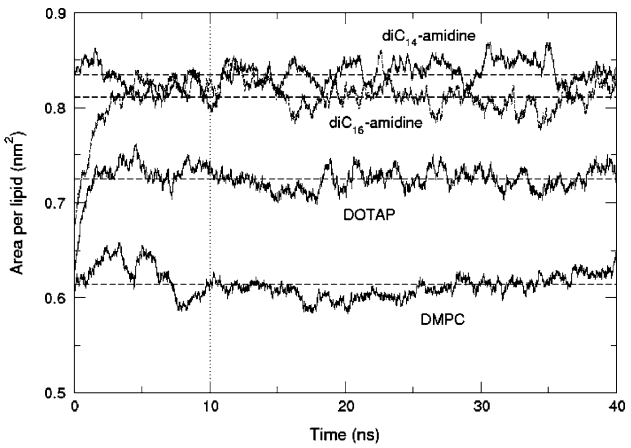

Fig. 7 Evolution of area per lipid during the course of the MD simulations. The area is calculated by dividing the system box *xy*-size by the number of lipids in a leaflet. Averages (*dashed lines*) for the region 10–40 ns are: DMPC: 0.61 nm^2; DOTAP: 0.72 nm^2; diC$_{14}$-amidine: 0.83 nm^2; diC$_{16}$-amidine: 0.81 nm^2

destabilize membranes, and are able to fuse with cells and enter efficiently and rapidly into cells, although they form stable liposomes by themselves under normal conditions.

Interestingly, by using molecular dynamics simulations, we demonstrated that cylindrically and conically shaped cationic lipids co-exist in the same bilayer (Fig. 8). This result is in apparent contradiction with a simple static description relying on the packing parameter P which considers that a stable bilayer is formed by cylindrically shaped lipids and that fusion can be induced only by adding conically shaped lipids to these bilayers [6, 13–15]. However, comparison of DMPC, DOTAP and diC$_{14}$, diC$_{16}$-amidine bilayer organizations revealed a tendency of diC$_{14}$ and diC$_{16}$-amidine towards conical structures (Fig. 8). Therefore, by comparing fusogenic behavior with lipid populations, we come to a more dynamic description where it is the excess of already existing V-shaped (conical) lipids that confers a tendency to fuse with cell membranes. It is possible that a threshold value for the ratio between cylindrically and conically shaped lipid structures exists, rather than the simple presence of V-shaped lipids, and below which the tendency to form conically shaped lipid structures shifts the liposomes into fusogenic behavior.

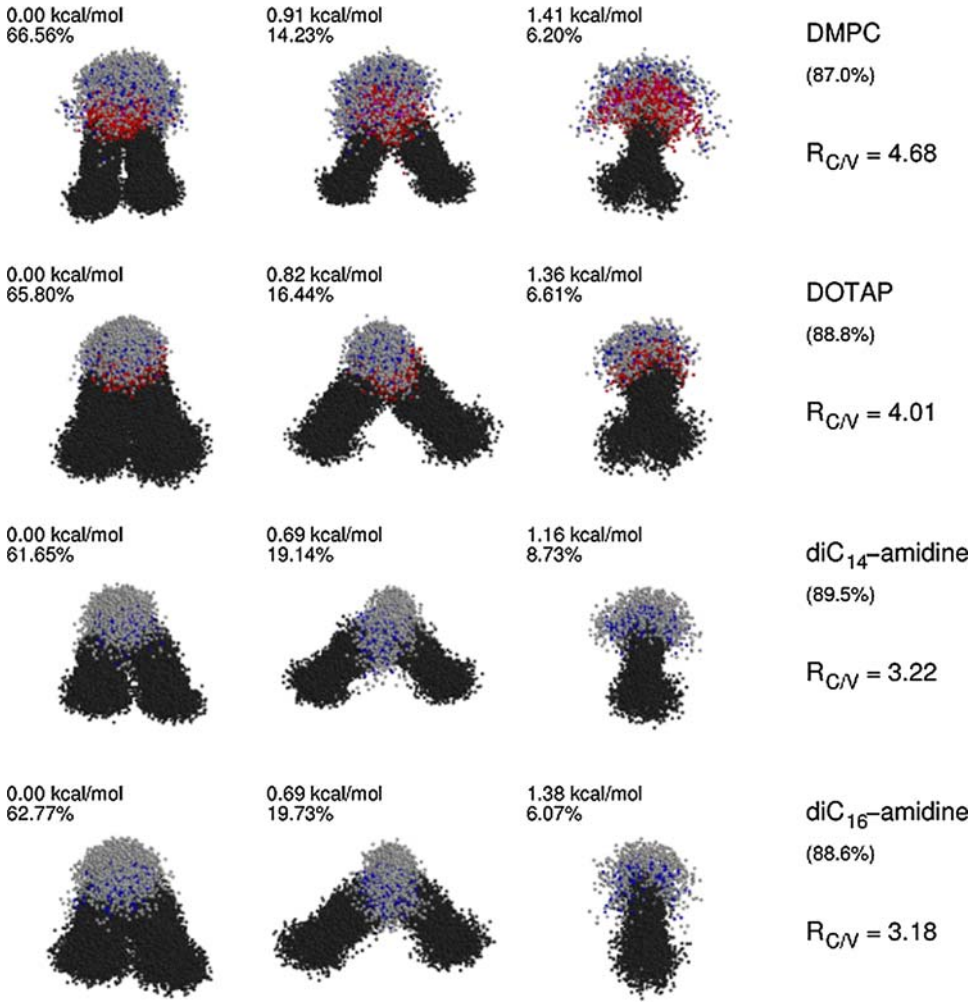

Fig. 8 Visualization of the three major clusters of the simulations: cylinder (*C*), cone (*V*) and twist (*T*). Clusters calculated as described in "Materials and Methods"

It is generally accepted that addition of a co-lipid (DOPE) to cationic lipid formulations improves in vitro transfection [7, 42], although the role of membrane fusion in this process was never clearly demonstrated. Fusion-promoting lipids such as DOPE are strong destabilizers for the lipid bilayer and can lead to membrane rupture as a side-event of fusion. When using cationic liposomes to deliver DNA or protein to cells, such a process might explain how a fraction of the liposomes and associated material might escape the endosomal compartment after capture [7, 9, 38]. Previous work using electron microscopy already suggested that rupture of the endocytic compartment occurs with different cationic liposomes, especially with diC_{14}-amidine [38]. Decomplexation of the transported DNA or protein, which is necessary for its availability as an active molecule inside the cell, might depend on dispersion and dilution of cationic lipids in the pool of intracellular membranes, a requirement that can be met by fusion with intracellular membrane followed by lateral diffusion of cationic lipids in the target membrane. Alternatively, it has been proposed that a shift of proton equilibrium towards the inner endosomal compartment, to compensate for the acid-buffering capacity of cationic lipids, could favor the entry of water as an osmotic response, ultimately resulting in the rupture of the endosomal membrane [43].

Surprisingly, fluorescently labeled diC_{14}-amidine lipids spread out in the cytoplasm very quickly (already seen after 5 min) after initial attachment of liposomes to a few localized spots on the cell surface (Fig. 4a). A possible scenario would imply intracellular transportation through endocytic vesicles followed by escape of a fraction of liposomes that fuse with many intracellular membrane targets. Contrary to what might be expected for such a quick and massive distribution of liposomal material throughout the cell, major cell functions remain intact even if cytokine secretion and signaling cascades can be modulated depending on the cationic lipid.

The dual and unexpected property of amidine cationic lipids to form stable liposomes in solution and their ability

to fuse with cellular membranes at physiological temperatures may lead to consider this class of cationic lipids as efficient vectors to insert missing components (like lipophilic drugs or membrane proteins—including receptors) into cellular membranes.

Acknowledgments C.L. is a Postdoctoral Researcher of the Belgian National Fund for Scientific research (FNRS), E.K. is a FRIA (Fonds pour la Formation à la Recherche dans l'Industrie et dans l'Agriculture) fellow, M.F.L. acknowledges support from the Walloon Region of Belgium—DGTRE contract 515993, and M.V. is a Research Associate of the Belgian National Fund for Scientific Research (FNRS). J.M.V. is Research Director of the National Fund for Scientific Research (Belgium) and acknowledges support from the National Fund for Scientific Research (Belgium), Télévie grant 7.4.558.07.F & Fonds de la Recherche Scientifique Médicale, grant 3.4.571.07.F

References

1. Felgner PL, Gadek TR, Holm M, Roman R, Chan HW, Wenz M, Northrop JP, Ringold GM, Danielsen M (1987) Lipofection: a highly efficient, lipid-mediated DNA-transfection procedure. Proc Natl Acad Sci USA 84:7413–7417
2. Wasungu L, Hoekstra D (2006) Cationic lipids, lipoplexes and intracellular delivery of genes. J Control Release 116:255–264
3. Elouahabi A, Ruysschaert JM (2005) Formation and intracellular trafficking of lipoplexes and polyplexes. Mol Ther 11:336–347
4. Zuhorn IS, Engberts JB, Hoekstra D (2007) Gene delivery by cationic lipid vectors: overcoming cellular barriers. Eur Biophys J 36:349–362
5. Wrobel I, Collins D (1995) Fusion of cationic liposomes with mammalian cells occurs after endocytosis. Biochim Biophys Acta 1235:296–304
6. Hafez IM, Cullis PR (2001) Roles of lipid polymorphism in intracellular delivery. Adv Drug Deliv Rev 47:139–148
7. Farhood H, Serbina N, Huang L (1995) The role of dioleoyl phosphatidylethanolamine in cationic liposome mediated gene transfer. Biochim Biophys Acta 1235:289–295
8. Zuhorn IS, Hoekstra D (2002) On the mechanism of cationic amphiphile-mediated transfection. To fuse or not to fuse: is that the question? J Membr Biol 189:167–179
9. Zuhorn IS, Bakowsky U, Polushkin E, Visser WH, Stuart MC, Engberts JB, Hoekstra D (2005) Nonbilayer phase of lipoplex-membrane mixture determines endosomal escape of genetic cargo and transfection efficiency. Mol Ther 11:801–810
10. Chernomordik LV, Zimmerberg J (1995) Bending membranes to the task: structural intermediates in bilayer fusion. Curr Opin Struct Biol 5:541–547
11. Cullis PR, Hope MJ (1978) Effects of fusogenic agent on membrane structure of erythrocyte ghosts and the mechanism of membrane fusion. Nature 271:672–674
12. Markin VS, Kozlov MM, Borovjagin VL (1984) On the theory of membrane fusion. The stalk mechanism. Gen Physiol Biophys 3:361–377
13. Ellens H, Bentz J, Szoka FC (1986) Destabilization of phosphatidylethanolamine liposomes at the hexagonal phase transition temperature. Biochemistry 25:285–294
14. Israelachvili JN, Mitchell DJ, Ninham BW (1976) Theory of self-assembly of hydrocarbon amphiphiles into micelles and bilayers. J Chem Soc Faraday Trans 272:1525–1568
15. Israelachvili JN (1994) Intermolecular and surface forces. Academic, London
16. Ruysschaert JM, el Ouahabi A, Willeaume V, Huez G, Fuks R, Vandenbranden M, Di Stefano P (1994) A novel cationic amphiphile for transfection of mammalian cells. Biochem Biophys Res Commun 203:1622–1628
17. Martin I, Ruysschaert J, Epand RM (1999) Role of the N-terminal peptides of viral envelope proteins in membrane fusion. Adv Drug Deliv Rev 38:233–255
18. Cladera J, Martin I, Ruysschaert JM, O'Shea P (1999) Characterization of the sequence of interactions of the fusion domain of the simian immunodeficiency virus with membranes. Role of the membrane dipole potential. J Biol Chem 274:29951–29959
19. Chattopadhyay A (1990) Chemistry and biology of *N*-(7-nitrobenz-2-oxa-1, 3-diazol-4-yl)-labeled lipids: fluorescent probes of biological and model membranes. Chem Phys Lipids 53:1–15
20. Titus JA, Haugland R, Sharrow SO, Segal DM (1982) Texas Red, a hydrophilic, red-emitting fluorophore for use with fluorescein in dual parameter flow microfluorometric and fluorescence microscopic studies. J Immunol Methods 50:193–204
21. Van Der Spoel D, Lindahl E, Hess B, Groenhof G, Mark AE, Berendsen HJ (2005) GROMACS: fast, flexible, and free. J Comput Chem 26:1701–1718
22. Kaminksi GA, Friesner RA, Tirado-Rives J, Jorgensen W (2001) Evaluation and Reparametrization of the OPLS-AA Force Field for Proteins via Comparison with Accurate Quantum Chemical Calculations on Peptides. J Phys Chem B 105:6474–6498
23. Berger O, Edholm O, Jahnig F (1997) Molecular dynamics simulations of a fluid bilayer of dipalmitoylphosphatidylcholine at full hydration, constant pressure, and constant temperature. Biophys J 72:2002–2013
24. Lensink MF, Lonez C, Ruysschaert JM, Vandenbranden M (2009) Characterization of the cationic DiC(14)-amidine bilayer by mixed DMPC/DiC(14)-amidine molecular dynamics simulations shows an interdigitated nonlamellar bilayer phase. Langmuir 25:5230–5238
25. Hess B (2007) P-LINCS: a parallel linear constraint solver for molecular simulation. J Chem Theory Comput 4:116–122
26. Guest MF, Bush IJ, Van Dam HJJ, Sherwood P, Thomas JMH, Van Lenthe JH, Havenith RWA, Kendrick J (2005) The GAMESS-UK electronic structure package: algorithms, developments and applications. Mol Phys Int J Interface Between Chem Phys 103:719–747
27. Bayly CI, Cieplak P, Cornell W, Kollman PA (2002) A well-behaved electrostatic potential based method using charge restraints for deriving atomic charges: the RESP model. J Phys Chem 97:10269–10280
28. Cornell WD, Cieplak P, Bayly CI, Gould IR, Merz KM, Ferguson DM, Spellmeyer DC, Fox T, Caldwell JW, Kollman PA (2002) A second generation force field for the simulation of proteins, nucleic acids, and organic molecules. J Am Chem Soc 117:5179–5197
29. Chandrasekhar J, Spellmeyer DC, Jorgensen WL (2002) Energy component analysis for dilute aqueous solutions of lithium(1+), sodium(1+), fluoride(1−), and chloride(1−) ions. J Am Chem Soc 106:903–910
30. Jorgensen WL, Madura JD (1985) Temperature and size dependence for Monte Carlo simulations of TIP4P water. Mol Phys Int J Interface Between Chem Phys 56:1381–1392
31. Bockmann RA, Hac A, Heimburg T, Grubmuller H (2003) Effect of sodium chloride on a lipid bilayer. Biophys J 85:1647–1655
32. Bockmann RA, Grubmuller H (2004) Multistep binding of divalent cations to phospholipid bilayers: a molecular dynamics study. Angew Chem Int Ed Engl 43:1021–1024
33. Gurtovenko AA (2005) Asymmetry of lipid bilayers induced by monovalent salt: atomistic molecular-dynamics study. J Chem Phys 122:244902

34. Cevc G (1990) Membrane electrostatics. Biochim Biophys Acta 1031:311–382
35. Daura X, Gademann K, Jaun B, Seebach D, van Gunsteren WF, Mark AE (1999) Peptide folding: when simulation meets experiment. Angew Chem Int Ed 38:236–240
36. Tandia BM, Lonez C, Vandenbranden M, Ruysschaert JM, Elouahabi A (2005) Lipid mixing between lipoplexes and plasma lipoproteins is a major barrier for intravenous transfection mediated by cationic lipids. J Biol Chem 280:12255–12261
37. Lonez C, Legat A, Vandenbranden M, Ruysschaert JM (2008) DiC14-amidine confers new anti-inflammatory properties to phospholipids. Cell Mol Life Sci 65:620–630
38. el Ouahabi A, Thiry M, Pector V, Fuks R, Ruysschaert JM, Vandenbranden M (1997) The role of endosome destabilizing activity in the gene transfer process mediated by cationic lipids. FEBS Lett 414:187–192
39. Kucerka N, Liu Y, Chu N, Petrache HI, Tristram-Nagle S, Nagle JF (2005) Structure of fully hydrated fluid phase DMPC and DLPC lipid bilayers using X-ray scattering from oriented multilamellar arrays and from unilamellar vesicles. Biophys J 88:2626–2637
40. Gurtovenko AA, Patra M, Karttunen M, Vattulainen I (2004) Cationic DMPC/DMTAP lipid bilayers: molecular dynamics study. Biophys J 86:3461–3472
41. Ellens H, Siegel DP, Alford D, Yeagle PL, Boni L, Lis LJ, Quinn PJ, Bentz J (1989) Membrane fusion and inverted phases. Biochemistry 28:3692–3703
42. Felgner JH, Kumar R, Sridhar CN, Wheeler CJ, Tsai YJ, Border R, Ramsey P, Martin M, Felgner PL (1994) Enhanced gene delivery and mechanism studies with a novel series of cationic lipid formulations. J Biol Chem 269:2550–2561
43. Boussif O, Lezoualc'h F, Zanta MA, Mergny MD, Scherman D, Demeneix B, Behr JP (1995) A versatile vector for gene and oligonucleotide transfer into cells in culture and in vivo: polyethylenimine. Proc Natl Acad Sci USA 92:7297–7301